

ON THE INFLUENCE OF WALL PROPERTIES IN THE PERISTALTIC MOTION OF MICROPOLAR FLUID

P. MUTHU¹, B. V. RATHISH KUMAR¹ and PEEYUSH CHANDRA¹

(Received 21 June, 2000; revised 6 September, 2001)

Abstract

We carry out a study of the peristaltic motion of an incompressible micropolar fluid in a two-dimensional channel. The effects of viscoelastic wall properties and micropolar fluid parameters on the flow are investigated using the equations of the fluid as well as of the deformable boundaries. A perturbation technique is used to determine flow characteristics. The velocity profile is presented and discussed briefly. We find the critical values of the parameters involving wall characteristics, which cause mean flow reversal.

1. Introduction

Expansion and contraction of an extensible tube in a fluid generate progressive waves which propagate along the length of the tube, mixing and transporting the fluid in the direction of wave propagation. This phenomenon is known as peristalsis. It is an inherent property of many tubular organs of the human body. In some biomedical instruments, such as heart-lung machines, peristaltic motion is used to pump blood and other biological fluids. It plays an indispensable role in transporting many physiological fluids in the body in various situations such as (i) urine transport from the kidney to the bladder through the ureter, (ii) transport of spermatozoa in the ductus efferentes of the male reproductive tract, (iii) movement of ovum in the fallopian tubes, (iv) vasomotion of small blood vessels, (v) mixing and transporting the contents of the gastrointestinal passage, and so forth. Peristaltic pumping mechanisms have been utilised for the transport of slurries, sensitive or corrosive fluids, sanitary fluid, noxious fluids in the nuclear industry, to name but a few examples. In some cases the transport of fluids is possible without moving internal mechanical components as is the case with peristaltically operated microelectromechanical system devices [18].

¹Department of Mathematics, Indian Institute of Technology, Kanpur 208 016, India;
e-mail: peeyush@iitk.ac.in.

The study of peristalsis in the context of fluid mechanics has received considerable attention in the last three decades mainly because of its relevance to biological systems and industrial applications. Several studies have been made analysing both theoretical and experimental aspects of the peristaltic motion of a Newtonian fluid [5, 8, 19, 24]. Numerical studies have also been reported in the literature [4, 17, 22, 23]. In these cases, the relevant fluid is assumed to be Newtonian. For a more detailed understanding of peristaltic transport, we refer to the review articles by Jaffrin and Shapiro [10] and Srivastava and Srivastava [21].

It is well-known that many physiological fluids behave in general like suspensions of deformable or rigid particles in a Newtonian fluid. Blood, for example, is a suspension of red cells, white cells and platelets in plasma. Another example is cervical mucus, which is a suspension of macromolecules in a water-like liquid. In view of this, some researchers have tried to account for the suspension behaviour of biofluids by considering them to be non-Newtonian [3, 15, 16, 20].

Eringen [7] introduced the concept of simple microfluids to characterise concentrated suspensions of neutrally buoyant deformable particles in a viscous fluid where the individuality of substructures affects the physical outcome of the flow. Such fluid models can be used to rheologically describe polymeric suspensions, normal human blood *etcetera* and have found applications in physiological and engineering problems [1, 2, 13]. A subclass of these microfluids is known as micropolar fluids where the fluid microelements are considered to be rigid [6]. Basically, these fluids can support couple stresses and body couples and exhibit microrotational and microinertial effects. The main advantage of using a micropolar fluid model to study the peristaltic flow of suspensions in comparison with other classes of non-Newtonian fluids is that it takes care of the rotation of fluid particles by means of an independent kinematic vector called the microrotation vector.

Girija Devi and Devanathan [9] studied the peristaltic motion of a micropolar fluid in a cylindrical tube with a sinusoidal wave of small amplitude travelling down its flexible wall for the case of low Reynolds number flow devoid of wall properties like tension and damping. However, consideration of wall properties is essential in various real situations. Mitra and Prasad [12] analysed the peristaltic motion of Newtonian fluid by considering the influence of the viscoelastic behaviour of walls. They assumed that the driving mechanism is in the form of a sinusoidal wave of moderate amplitude imposed on the flexible walls of the channel. Dynamic boundary conditions were proposed for the fluid motion due to the symmetric motion of the flexible walls which were assumed to be either thin elastic plates or membranes [12]. The present study attempts to understand the influence of sinusoidally varying walls on the peristaltic motion of micropolar fluid in a channel using the dynamic boundary condition. Using perturbation techniques, analytical approximate solutions for the stream function and microrotation velocity have been obtained as a power series in terms of the small

amplitude ratio. Results are discussed for various parameters of the flow and are depicted graphically.

2. Mathematical model and the governing equations

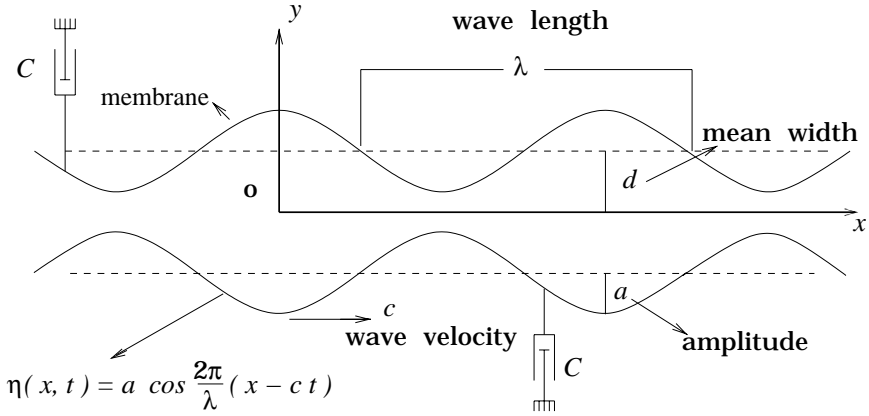


FIGURE 1. Geometry of a two-dimensional peristaltic channel

Consider a two-dimensional symmetric flow of unsteady incompressible micropolar fluid in an infinite channel of uniform thickness $2d$, with a sinusoidal wave travelling along the walls of the channel with speed c , small amplitude a and long wave length λ (see Figure 1). The walls are assumed to be flexible membranes. The governing equations for the peristaltic motion of an incompressible micropolar fluid are given in Cartesian form (by neglecting the body forces and body couples) [14] as

$$\frac{\partial u}{\partial x} + \frac{\partial v}{\partial y} = 0, \quad (2.1)$$

$$\rho \left[\frac{\partial u}{\partial t} + u \frac{\partial u}{\partial x} + v \frac{\partial u}{\partial y} \right] = -\frac{\partial p}{\partial x} + \left(\frac{2\mu + \kappa}{2} \right) \nabla^2 u + \kappa \frac{\partial v}{\partial y}, \quad (2.2)$$

$$\rho \left[\frac{\partial v}{\partial t} + u \frac{\partial v}{\partial x} + v \frac{\partial v}{\partial y} \right] = -\frac{\partial p}{\partial y} + \left(\frac{2\mu + \kappa}{2} \right) \nabla^2 v - \kappa \frac{\partial v}{\partial x}, \quad (2.3)$$

$$\rho J \left[\frac{\partial v}{\partial t} + u \frac{\partial v}{\partial x} + v \frac{\partial v}{\partial y} \right] = -2\kappa v + \gamma \nabla^2 v + \kappa \left[\frac{\partial v}{\partial x} - \frac{\partial u}{\partial y} \right], \quad (2.4)$$

where $u(x, y, t)$ and $v(x, y, t)$ are the velocity components in the x and y directions respectively, $v(x, y, t)$ is the microrotation velocity component in the direction normal to both the x and y axes and the origin is taken at the centre line of the channel (Figure 1). Here J is the microinertia constant, μ is the viscosity coefficient of

classical fluid dynamics, κ and γ are the new viscosity coefficients for the micropolar fluids, ρ is the density of the fluid and $\nabla^2 \equiv \partial^2/\partial x^2 + \partial^2/\partial y^2$.

The displacement ($\eta(x, t)$) of the wall of the channel is given by

$$\eta(x, t) = a \cos(2\pi(x - ct)/\lambda).$$

We assume that the walls are inextensible so that only lateral motion takes place and the horizontal displacement of the wall is zero.

Thus the no-slip boundary conditions for the velocity and microrotation are

$$u = 0, \quad v = 0$$

at $y = \pm(d + \eta(x, t))$.

It may be mentioned that the main purpose of the present study is to understand the dynamic interaction of the fluid and the walls in peristalsis. So the dynamic boundary conditions are imposed on the fluid by the symmetric motion of the flexible walls, which, following Mittra and Prasad [12], can be written as

$$\frac{\partial L(\eta)}{\partial x} = -\rho \left[\frac{\partial u}{\partial t} + u \frac{\partial u}{\partial x} + v \frac{\partial u}{\partial y} \right] + \left(\frac{2\mu + \kappa}{2} \right) \nabla^2 u + \kappa \frac{\partial v}{\partial y}$$

at $y = \pm(d + \eta(x, t))$, where

$$\frac{\partial L(\eta)}{\partial x} = -T \frac{\partial^3 \eta}{\partial x^3} + m \frac{\partial^3 \eta}{\partial t^2 \partial x} + C \frac{\partial^2 \eta}{\partial t \partial x}. \quad (2.5)$$

Here T is the tension in the membrane, m is the mass per unit area and C is the coefficient of viscous damping force.

Introducing the stream function, Ψ , in terms of

$$u = \frac{\partial \Psi}{\partial y}, \quad v = -\frac{\partial \Psi}{\partial x} \quad (2.6)$$

and eliminating the pressure between (2.2) and (2.3), we get differential equations for Ψ and v . Using d and c as the characteristic length and characteristic velocity, these equations are non-dimensionalised by introducing the following non-dimensional variables:

$$\begin{aligned} x' &= \frac{x}{d}, & y' &= \frac{y}{d}, & t' &= \frac{tc}{d}, & u' &= \frac{u}{c}, & v' &= \frac{v}{c}, \\ v' &= \frac{vd}{c}, & p' &= \frac{p}{\rho c^2}, & \eta' &= \frac{\eta}{d}, & \Psi' &= \frac{\Psi}{cd}, & J' &= \frac{J}{d^2}. \end{aligned}$$

After non-dimensionalisation, the accents are dropped and the governing equations and boundary conditions, in non-dimensional form, are written as

$$\frac{\partial}{\partial t} \nabla^2 \Psi + \Psi_y \nabla^2 \Psi_x - \Psi_x \nabla^2 \Psi_y = \frac{2 + \mu_1}{2R_e} [\nabla^2 \nabla^2 \Psi] + \frac{\mu_1}{R_e} \nabla^2 v, \quad (2.7)$$

$$R_l \left(\frac{\partial v}{\partial t} + \Psi_y \frac{\partial v}{\partial x} - \Psi_x \frac{\partial v}{\partial y} \right) = 2(1 - N^2) [\nabla^2 v] - N^2 M^2 [\nabla^2 \Psi + 2v]. \quad (2.8)$$

The boundary conditions at $y = \pm(1 + \eta(x, t))$ are

$$\begin{aligned} \Psi_y &= 0, \quad v = 0, \\ \frac{\partial L(\eta)}{\partial x} &= -[\Psi_{y_t} + \Psi_y \Psi_{xy} - \Psi_x \Psi_{yy}] + \frac{2 + \mu_1}{2R_e} [\nabla^2 \Psi_y] + \frac{\mu_1}{R_e} \frac{\partial v}{\partial y}, \end{aligned} \quad (2.9)$$

where

$$\frac{\partial L(\eta)}{\partial x} = -\frac{K_3}{R_e^2} \frac{\partial^3 \eta}{\partial x^3} + m_1 \frac{\partial^3 \eta}{\partial t^2 \partial x} + \frac{K_2}{R_e} \frac{\partial^2 \eta}{\partial t \partial x},$$

$\eta(x, t) = \epsilon \cos(\alpha(x - t))$, $\epsilon = a/d$, $\alpha = 2\pi d/\lambda$, $R_e = \rho c d/\mu$, $\mu_1 = \kappa/\mu$ and

$$\begin{aligned} N &= \left(\frac{\mu_1}{2 + \mu_1} \right)^{1/2}, \quad M = 2d \left(\frac{\mu}{\gamma} \right)^{1/2}, \quad K_2 = \frac{Cd}{\mu}, \\ K_3 &= \frac{T\rho d}{\mu^2}, \quad m_1 = \frac{m}{\rho d}, \quad R_l = \frac{8\mu\rho c d J}{\gamma(2\mu + \kappa)}. \end{aligned}$$

The parameters ϵ , α and R_e are the amplitude ratio, wave number and Reynolds number respectively. These are the usual fundamental quantities observed in classical peristaltic flow [8, 12]. The parameters μ_1 and M are non-dimensional quantities due to micropolar fluid flow. Also μ_1 denotes the ratio of the viscosity coefficient for micropolar fluids and the classical viscosity coefficient. It characterises the coupling of (2.7) and (2.8). The parameter M can be thought of as a fluid property depending upon the size of the microstructure. This is due to the factor $(\gamma/\mu)^{1/2}$, which has the dimension of length. It can be noted that as κ tends to zero, μ_1 becomes zero and (2.7) and (2.8) are uncoupled. Further, when κ and γ are zero, that is, when μ_1 becomes zero and M tends to infinity, (2.7) and (2.8) reduce to the classical Navier-Stokes equations. We note that R_l is the modified Reynolds number and involves the quantity J (microinertia constant), where J is the square of a length typical of microstructure, and it is reasonable to assume that $R_l \ll 1$ [11, 14]. In view of this, the effect of microinertia is neglected and R_l is taken to be zero in the following analysis.

The parameters K_2 , K_3 and m_1 are the non-dimensional quantities related to the wall motion through the dynamic boundary condition (2.9). The parameters K_2 and K_3 respectively represent the dissipative and rigiditive feature of walls, whereas

m_1 indicates the stiffness property of walls. The choice $K_2 = 0$ implies that the walls move up and down with no damping force on them and hence indicates the case of elastic walls. The rigid nature of the walls is represented by K_3 , which depends upon the wall tension.

3. Analysis

It may be noted that the flow is quite complex because of nonlinearity and the coupled behaviour of the governing equations and the boundary conditions. Thus to solve (2.7) and (2.8) for the velocity field and microrotation, we attempt an approximate solution as a power series in terms of ϵ (ratio of amplitude to mean breadth of the wavy wall). The pressure gradient is taken as

$$\frac{\partial p}{\partial x} = \left(\frac{\partial p}{\partial x}\right)_0 + \epsilon \left(\frac{\partial p}{\partial x}\right)_1 + \epsilon^2 \left(\frac{\partial p}{\partial x}\right)_2 + \dots .$$

Further, it may be pointed out here that although the peristaltic motion is caused by a single harmonic wave, the velocity field will consist of all harmonics due to the nonlinearity of the equations. Thus we assume Ψ and v are given in the following form:

$$\begin{aligned} \Psi = & \Psi_0(y) + \frac{\epsilon}{2} (\phi_1(y)e^{i\alpha(x-t)} + \phi_1^*(y)e^{-i\alpha(x-t)}) \\ & + \frac{\epsilon^2}{2} (\phi_{20}(y) + \phi_{22}(y)e^{2i\alpha(x-t)} + \phi_{22}^*(y)e^{-2i\alpha(x-t)}) + o(\epsilon^3), \end{aligned} \tag{3.1}$$

$$\begin{aligned} v = & v_0(y) + \frac{\epsilon}{2} (\xi_1(y)e^{i\alpha(x-t)} + \xi_1^*(y)e^{-i\alpha(x-t)}) \\ & + \frac{\epsilon^2}{2} (\xi_{20}(y) + \xi_{22}(y)e^{2i\alpha(x-t)} + \xi_{22}^*(y)e^{-2i\alpha(x-t)}) + o(\epsilon^3). \end{aligned} \tag{3.2}$$

Here the asterisk denotes complex conjugate and $\Psi_0(y)$ and $v_0(y)$ correspond to the plane Poiseuille flow, where $\epsilon = 0$. Substituting (3.1) and (3.2) in (2.7) to (2.9) and collecting the terms of various powers of ϵ and also different harmonics, we get the differential equations for different orders of Ψ and v (Appendix A).

Since zeroth-order differential equations correspond to plane Poiseuille flow of micropolar fluid, where $\epsilon = 0$, the equations can be easily solved along with the corresponding boundary conditions for Ψ_0 and v_0 with a constant pressure gradient $(dp/dx)_0$. Thus we get

$$\begin{aligned} \frac{d\Psi_0}{dy} = & K(y^2 - 1) + 2K \frac{N}{M} \left(\frac{\cosh(NM) - \cosh(NMy)}{\sinh(NM)} \right), \\ v_0 = & K \left(\frac{\sinh(NMy) - y \sinh(NM)}{\sinh(NM)} \right), \end{aligned}$$

where $K = (R_e/(2 + \mu_1))(dp/dx)_0$ is the Poiseuille flow parameter for the micropolar fluid.

For pure peristalsis (free pumping), which means that the flow is generated by wall motions only, the pressure gradient $(\partial p/\partial x)_0 = 0$. This implies that $K = 0$, which gives $\Psi_0(y) \equiv 0$, $v_0(y) \equiv 0$.

The time mean flow $\bar{u}(y)$ is defined as the velocity averaged over the period of oscillation (τ) of the wave propagation imposed on the flexible walls,

$$\bar{u}(y) = \frac{1}{\tau} \int_{t=0}^{\tau} \frac{\partial \Psi}{\partial y} dt = \Psi_0^{(1)}(y) + \frac{\epsilon^2}{2} \phi_{20}^{(1)}(y) + o(\epsilon^3).$$

Here $f^{(2)}$ means $d^2 f/dy^2$. In the following we shall discuss the case of free pumping only. In that case, we have

$$\bar{u}(y) = \frac{\epsilon^2}{2} \phi_{20}^{(1)}(y) + o(\epsilon^3). \quad (3.3)$$

It is clear from the equations corresponding to the order of ϵ^2 that to calculate ϕ_{20} for the free pumping case, we need the expression for ϕ_1 and ξ_1 . The governing equations for ϕ_1 and ξ_1 for the free pumping case reduce to

$$\begin{aligned} (\phi_1^{(4)} - 2\alpha^2 \phi_1^{(2)} + \alpha^4 \phi_1) + 2\mu_1 (\xi_1^{(2)} - \alpha^2 \xi_1) &= \frac{2i\alpha R_e}{2 + \mu_1} (\alpha^2 \phi_1 - \phi_1^{(2)}), \\ 2(1 - N^2) (\xi_1^{(2)} - \alpha^2 \xi_1) - 2N^2 M^2 \xi_1 - N^2 M^2 (\phi_1^{(2)} - \alpha^2 \phi_1) &= 0 \end{aligned} \quad (3.4)$$

and the boundary conditions are

$$\begin{aligned} \phi_1^{(1)}(\pm 1) &= 0, \quad \xi_1(\pm 1) = 0, \\ \phi_1^{(3)}(\pm 1) + 2\mu_1 \xi_1^{(1)}(\pm 1) &= \frac{2R_e \delta_1}{2 + \mu_1}, \end{aligned} \quad (3.5)$$

where $\delta_1 = i(K_3 \alpha^3/R_e^2 - m_1 \alpha^3) + K_2 \alpha^2/R_e$.

It is clear from (3.3) that to determine $\bar{u}(y)$ up to the second order of ϵ , we need the expression for ϕ_{20} . Thus in the following we give the equations governing ϕ_{20} only, for the case of free pumping,

$$\begin{aligned} \phi_{20}^{(4)} + 2\mu_1 \xi_{20}^{(2)} &= \frac{-i\alpha R_e}{(2 + \mu_1)} (\phi_1 \phi_1^{*(2)} - \phi_1^* \phi_1^{(2)})^{(1)}, \\ 2(1 - N^2) \xi_{20}^{(2)} - 2N^2 M^2 \xi_{20} - N^2 M^2 \phi_{20}^{(2)} &= 0, \end{aligned} \quad (3.6)$$

with boundary conditions

$$\phi_{20}^{(1)}(\pm 1) = \mp \frac{1}{2} (\phi_1^{(2)}(\pm 1) + \phi_1^{*(2)}(\pm 1)), \quad \xi_{20}(\pm 1) = \mp \frac{1}{2} (\xi_1^{(1)}(\pm 1) + \xi_1^{*(1)}(\pm 1)),$$

and

$$\begin{aligned}
 & \phi_{20}^{(3)}(\pm 1) + 2\mu_1 \xi_{20}^{(1)}(\pm 1) \\
 &= \pm \frac{i\alpha R_e}{(2 + \mu_1)} (\phi_1^{*(2)}(\pm 1) - \phi_1^{(2)}(\pm 1)) \pm \frac{\alpha^2}{2} (\phi_1^{(2)}(\pm 1) + \phi_1^{*(2)}(\pm 1)) \\
 &\mp \frac{1}{2} (\phi_1^{(4)}(\pm 1) + \phi_1^{*(4)}(\pm 1)) \\
 &\quad - \frac{i\alpha R_e}{(2 + \mu_1)} (\phi_1(\pm 1)\phi_1^{*(2)}(\pm 1) - \phi_1^*(\pm 1)\phi_1^{(2)}(\pm 1)) \\
 &\mp N^2 (\xi_1^{(2)}(\pm 1) + \xi_1^{*(2)}(\pm 1)). \tag{3.7}
 \end{aligned}$$

Solutions for $\phi_1(y)$, $\xi_1(y)$ and $\phi_{20}(y)$ are given in Appendix B and $\bar{u}(y)$ is calculated from (3.3).

4. Numerical results and discussion

In the following we study the effects of various parameters on the time mean flow for the case of pure peristalsis only. The time mean flow, $\bar{u}(y)$, approximated up to order ϵ^2 , is given by (3.3). It may be noted that, apart from the usual dimensionless parameters of peristaltic flow, R_e (Reynolds number), α (wave number) and ϵ (amplitude ratio), in this case the flow also depends upon the following non-dimensional quantities:

- (1) the micropolar fluid parameters μ_1 and M ; and
- (2) the wall parameters K_2 , K_3 and m_1 , which describe the viscoelastic behaviour of the flexible walls.

We mention here that μ_1 and M characterise the coefficient of viscosity (κ) and of gyroviscosity (γ) respectively. An increase in κ is reflected in the coupling parameter μ_1 , while an increase in γ results in decreasing values of M . Also the expression for $\bar{u}(y)$ reduces to the Newtonian case [12], as $\mu_1 \rightarrow 0$ and $M \rightarrow \infty$.

The parameters K_2 and K_3 represent respectively the dissipative and rigiditive features of the walls while m_1 indicates the stiffness property of the walls. The choice $K_2 = 0$ implies that the walls move up and down with no damping force on them and hence indicates the case of elastic walls. The rigid nature of the walls is represented by K_3 . In our analysis we assume that there is no stiffness in the walls and this implies $m_1 = 0$. It may be noted from (2.5) that these three quantities cannot be taken as zero simultaneously.

We shall now consider the following two cases for the wall properties:

- (i) elastic wall ($K_2 = 0$);
- (ii) dissipative wall ($K_2 \neq 0$).

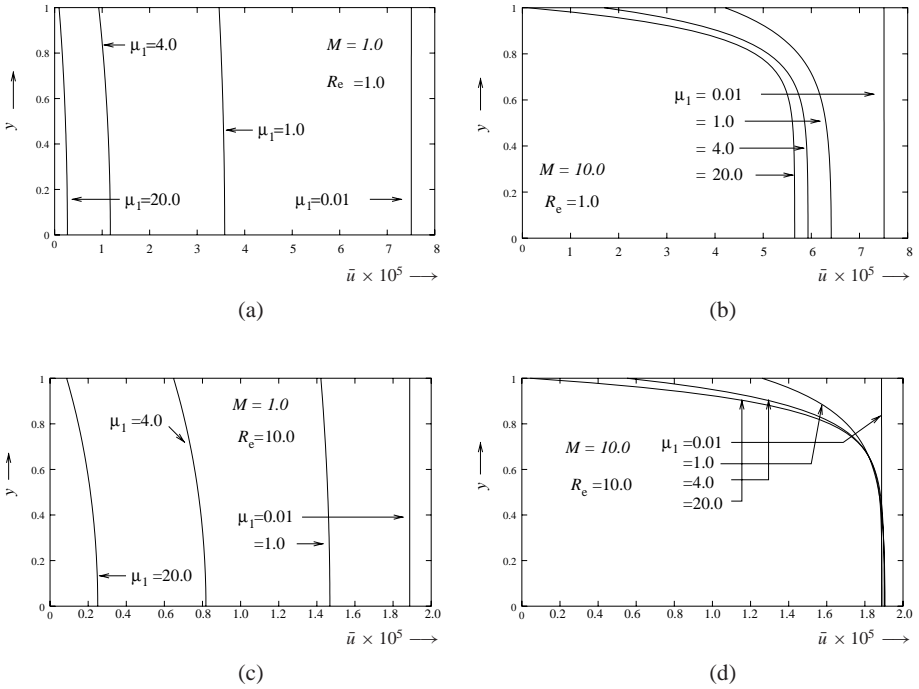


FIGURE 2. Distribution of \bar{u} with y for $\alpha = 0.5$ ($K_2 = 0, K_3 = 1.0, m_1 = 0$)

Case (i): $K_2 = 0$. This corresponds to elastic walls where the dissipative effects are neglected. In this case we numerically study the effects of fluid parameters and α (wave number) on the mean flow characteristics, by taking $K_3 = 1.0$ and $m_1 = 0.0$ in a channel where $\epsilon = 0.1$.

Figures 2 and 3 show the effect of μ_1, M and R_e on the time mean flow, induced by the travelling waves on the flexible walls, when $\alpha = 0.5$ and $\alpha = 2.0$ respectively.

The effect of γ (the coefficient of gyroviscosity) is observed by comparing the graphs for $M = 1$ (Figures 2 (a), (c) and 3 (a), (c)) and for $M = 10$ (Figures 2 (b), (d) and 3 (b), (d)). It is seen here that $\bar{u}(y)$ is large for higher values of M ($M = 10$). Further, when $M = 1$, the flow is almost like a plug flow and $\bar{u}(y)$ is almost constant. However, for $M = 10$, the plug flow is observed in most parts of the channel and $\bar{u}(y)$ sharply decreases to zero near the walls. In the case where $M = 10$, the variation with respect to μ_1 is not very significant.

To see the influence of the Reynolds number (R_e), we have considered the two cases $R_e = 1$ and $R_e = 10$. It is seen that $\bar{u}(y)$ decreases as R_e increases. Further, it is observed that while the qualitative behaviour of $\bar{u}(y)$ with respect to μ_1 and M remains similar in the two cases for R_e , the effect of μ_1 is more significant at low Reynolds number, when $M = 10$.

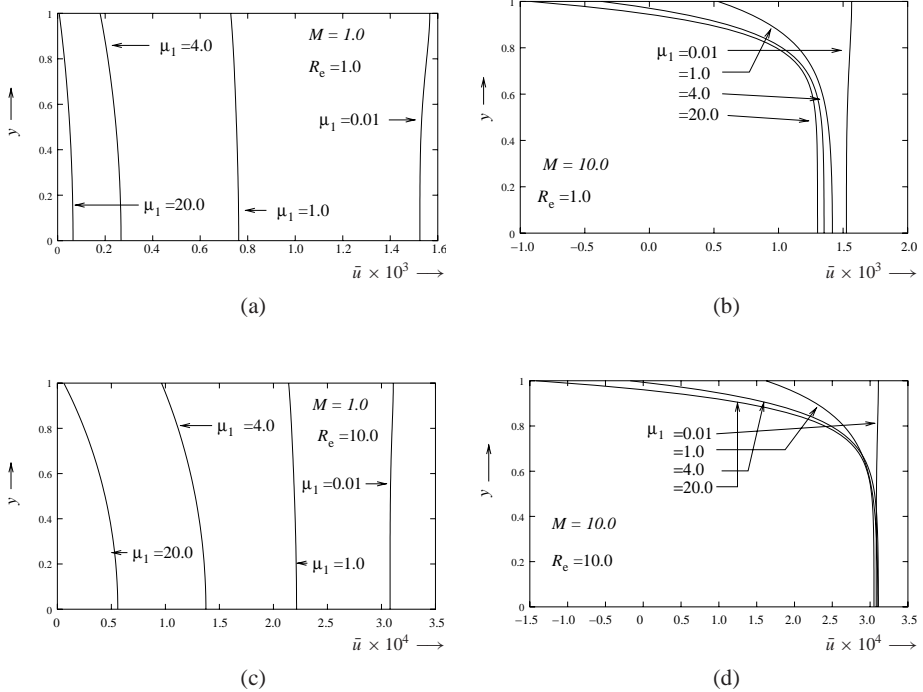


FIGURE 3. Distribution of \bar{u} with y for $\alpha = 2.0$ ($K_2 = 0, K_3 = 1.0, m_1 = 0$)

The same analysis is repeated with $\alpha = 2.0$. The pictorial representation for this analysis is given in Figure 3. Comparing Figures 2 and 3, it is observed that $\bar{u}(y)$ increases with an increase in α .

In Figure 4, we see the effect of K_3 on $\bar{u}(y)$ for the case of pure peristalsis with elastic walls ($K_2 = 0$), by taking $\alpha = 1, R_e = 10$ and $m_1 = 0$. It is observed that as K_3 increases, $\bar{u}(1)$ increases and $\bar{u}(0)$ decreases. In fact $\bar{u}(y)$ remains positive throughout the channel until K_3 attains a critical value K_{3c} , for which $\bar{u}(0) = 0$, and after that it starts showing flow reversal behaviour at the middle of the channel, that is, when $y = 0$. It is seen from Figure 4 that the value of K_{3c} depends upon μ_1 and M . It increases as μ_1 increases and decreases with M . As larger values of K_3 correspond to higher rigidity of the flexible boundary walls, one can conclude that higher rigidity of the walls is required for mean flow reversal to take place in the case of micropolar fluids.

Case (ii): Dissipative wall ($K_2 \neq 0$). In the next two figures (5 and 6), we see the effect of the dissipative nature of the walls ($K_2 \neq 0$) on the flow reversal by taking $K_3 = 1$ and $m_1 = 0$. To see this effect, $\bar{u}(1)$, that is, time mean flow at the boundary is plotted versus α (wave number). While it is observed that no flow reversal takes

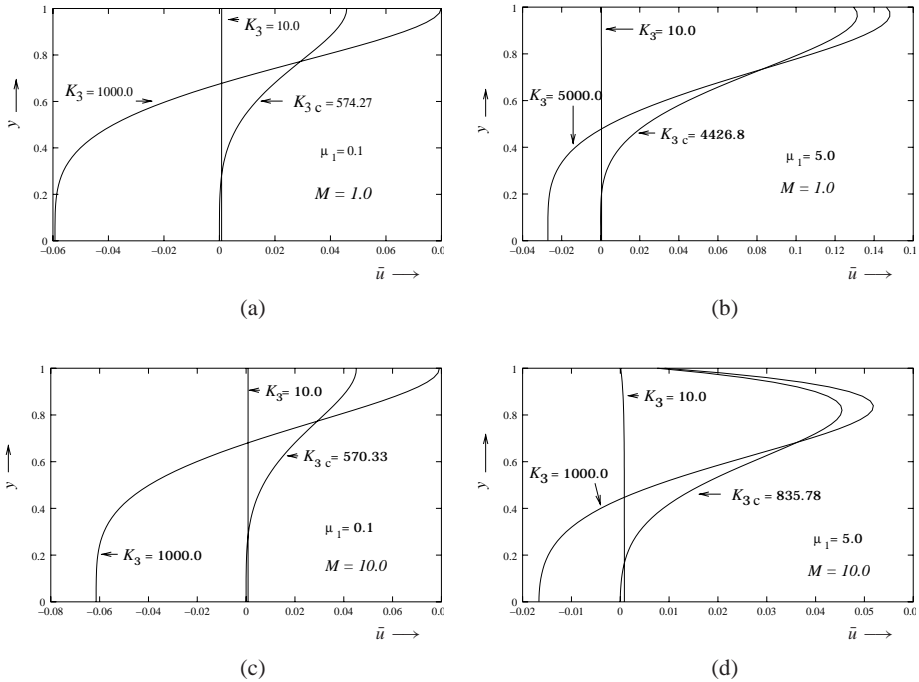


FIGURE 4. Mean velocity distribution for $\alpha = 1.0$, $R_e = 10.0$ ($K_2 = 0$, $m_1 = 0$)

place at the boundary for smaller values of K_2 ($M = 1$, Figure 5), for any value of α , $\bar{u}(1)$ is negative for larger values of K_2 and it keeps on decreasing as α increases.

Thus the dissipative nature of the walls causes flow reversal at the boundary. This is observed for various values of μ_1 , M and R_e . We note that in the case of non-dissipative walls this phenomenon was not observed. The effect of the coupling parameter μ_1 is to decrease the values of $\bar{u}(1)$ and the effect of M is not very significant (Figures 5 (a) and 6 (a)). The effect of R_e is to decrease the value of $\bar{u}(1)$ at small values of K_2 and α . At large values of K_2 the reverse effect is observed at all values of α , except in the case of $\mu_1 = 10$ and $M = 10$ (Figure 6 (b)). This peculiar behaviour of $\bar{u}(1)$ (Figure 6 (b)) is due to the combined effect of μ_1 and R_e as $\bar{u}(1)$ decreases with μ_1 and increases with R_e for larger value of K_2 .

5. Conclusion

In the present study an analysis of peristaltic transport of a micropolar fluid in a channel with dynamic boundary conditions has been presented. It is observed that $\bar{u}(y)$ decreases when μ_1 increases and as M decreases. The phenomenon of flow

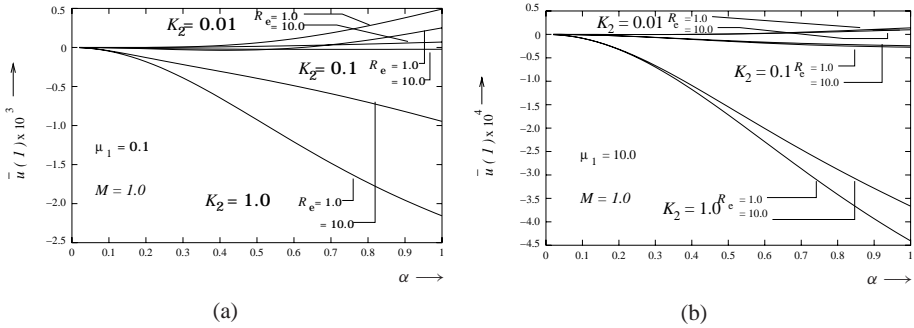


FIGURE 5. Effect of viscous damping on $\bar{u}(1)$ ($K_3 = 1.0$, $m_1 = 0.0$)

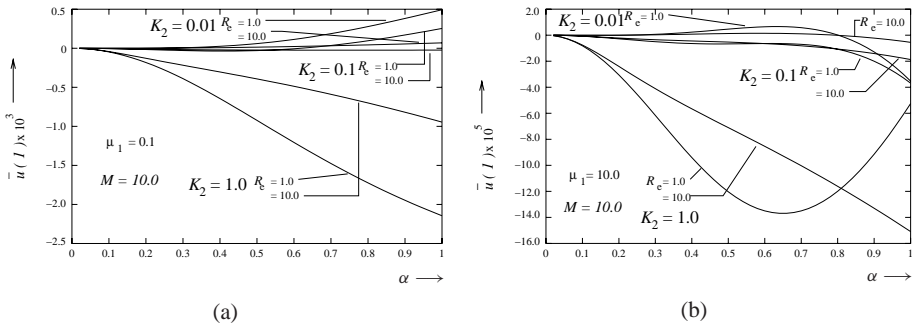


FIGURE 6. Effect of viscous damping on $\bar{u}(1)$ ($K_3 = 1.0$, $m_1 = 0.0$)

reversal takes place in the centerline of the channel due to rigidity variation in the boundary walls, when viscous damping is zero. The critical value of K_3 increases with an increase in μ_1 and it decreases as M increases. For non-zero viscous damping, flow reversal is found at the channel walls. Furthermore, these flow variables approach behaviour in accordance with classical theory as the microstructure loses its behaviour.

Acknowledgement. The authors are thankful to the referees for their constructive remarks.

Appendix A.

The governing equations for Ψ_0 and v_0 are

$$\begin{aligned} (2 + \mu_1)\Psi_0^{(4)} + 2\mu_1v_0^{(2)} &= 0, \\ 2(1 - N^2)[v_0^{(2)}] - N^2M^2[\Psi_0^{(2)} + 2v_0] &= 0, \end{aligned}$$

with boundary conditions given by $\Psi_0^{(1)}(\pm 1) = 0$, $v_0(\pm 1) = 0$. The governing equations for ϕ_1 and ξ_1 are

$$\begin{aligned} & \frac{2 + \mu_1}{2R_e} (\phi_1^{(4)} - 2\alpha^2 \phi_1^{(2)} + \alpha^4 \phi_1) + \frac{\mu_1}{R_e} (\xi_1^{(2)} - \alpha^2 \xi_1) \\ & = i\alpha (1 - \Psi_0^{(1)}) (\alpha^2 \phi_1 - \phi_1^{(2)}) - i\alpha \Psi_0^{(3)} \phi_1, \\ & 2(1 - N^2) (\xi_1^{(2)} - \alpha^2 \xi_1) - 2N^2 M^2 \xi_1 - N^2 M^2 (\phi_1^{(2)} - \alpha^2 \phi_1) = 0, \end{aligned}$$

with boundary conditions given by

$$\begin{aligned} & \phi_1^{(1)}(\pm 1) = \mp \Psi_0^{(2)}(\pm 1), \quad \xi_1(\pm 1) = \mp v_0^{(1)}(\pm 1), \\ & \frac{2 + \mu_1}{2R_e} (\phi_1^{(3)}(\pm 1) - \alpha^2 \phi_1^{(1)}(\pm 1) \pm \Psi_0^{(4)}(\pm 1)) + i\alpha \phi_1^{(1)}(\pm 1) (1 - \Psi_0^{(1)}(\pm 1)) \\ & + i\alpha \phi_1(\pm 1) \Psi_0^{(2)}(\pm 1) + \frac{\mu_1}{R_e} (\xi_1^{(1)}(\pm 1) \pm v_0^{(2)}(\pm 1)) = \delta_1, \end{aligned}$$

where $\delta_1 = i(K_3 \alpha^3 / R_e^2 - m_1 \alpha^3) + K_2 \alpha^2 / R_e$. The governing equations for ϕ_{20} and ξ_{20} are

$$\begin{aligned} & \frac{2 + \mu_1}{2R_e} \phi_{20}^{(4)} + \frac{\mu_1}{R_e} \xi_{20}^{(2)} = \frac{-i\alpha}{2} (\phi_1 \phi_1^{*(2)} - \phi_1^* \phi_1^{(2)})^{(1)}, \\ & 2(1 - N^2) \xi_{20}^{(2)} - 2N^2 M^2 \xi_{20} - N^2 M^2 \phi_{20}^{(2)} = 0, \end{aligned}$$

with boundary conditions given by

$$\begin{aligned} & \phi_{20}^{(1)}(\pm 1) = \mp \frac{1}{2} (\phi_1^{(2)}(\pm 1) + \phi_1^{*(2)}(\pm 1)) - \frac{1}{2} \Psi_0^{(3)}(\pm 1), \\ & \xi_{20}(\pm 1) = \mp \frac{1}{2} (\xi_1^{(1)}(\pm 1) + \xi_1^{*(1)}(\pm 1)) - \frac{1}{2} v_0^{(2)}(\pm 1), \\ & \phi_{20}^{(3)}(\pm 1) + \mu_1 \xi_{20}^{(1)}(\pm 1) = \pm \frac{i\alpha R_e}{(2 + \mu_1)} (\phi_1^{*(2)}(\pm 1) - \phi_1^{(2)}(\pm 1)) \\ & \quad \pm \frac{\alpha^2}{2} (\phi_1^{(2)}(\pm 1) + \phi_1^{*(2)}(\pm 1)) \mp \frac{1}{2} (\phi_1^{(4)}(\pm 1) + \phi_1^{*(4)}(\pm 1)) \\ & \quad - \frac{1}{2} \Psi_0^{(5)}(\pm 1) \pm \frac{i\alpha R_e}{(2 + \mu_1)} \Psi_0^{(3)}(\pm 1) (\phi_1^*(\pm 1) - \phi_1(\pm 1)) \\ & \quad - \frac{i\alpha R_e}{(2 + \mu_1)} (\phi_1(\pm 1) \phi_1^{*(2)}(\pm 1) - \phi_1^*(\pm 1) \phi_1^{(2)}(\pm 1)) \\ & \quad \mp N^2 (\xi_1^{(2)}(\pm 1) + \xi_1^{*(2)}(\pm 1)) - N^2 v_0^{(2)}(\pm 1). \end{aligned}$$

The governing equations for ϕ_{22} and ξ_{22} are

$$\begin{aligned} & \frac{2 + \mu_1}{2R_e} (\phi_{22}^{(4)} - 8\alpha^2 \phi_{22}^{(2)} + 16\alpha^4 \phi_{22}) + \frac{\mu_1}{R_e} (\xi_{22}^{(2)} - 4\alpha^2 \xi_{22}) \\ & = 2i\alpha (1 - \Psi_0^{(1)}) (4\alpha^2 \phi_{22} - \phi_{22}^{(2)}) - 2i\alpha \Psi_0^{(3)} \phi_{22} + \frac{i\alpha}{2} (\phi_1^{(1)} \phi_1^{(2)} - \phi_1 \phi_1^{(3)}), \end{aligned}$$

$$2(1 - N^2) (\xi_{22}^{(2)} - 4\alpha^2 \xi_{22}) - 2N^2 M^2 \xi_{22} - N^2 M^2 (\phi_{22}^{(2)} - 4\alpha^2 \phi_{22}) = 0,$$

with boundary conditions given by

$$\begin{aligned} \phi_{22}^{(1)}(\pm 1) &= \mp \phi_1^{(2)}(\pm 1)/2 - \Psi_0^{(3)}(\pm 1)/4, \\ \xi_{22}(\pm 1) &= \mp \xi_1^{(1)}(\pm 1)/2 - \nu_0^{(2)}(\pm 1)/4, \\ \frac{2 + \mu_1}{2R_e} \phi_{22}^{(3)}(\pm 1) + (2i\alpha - \frac{2(2 + \mu_1)\alpha^2}{R_e}) \phi_{22}^{(1)}(\pm 1) \\ &+ 2i\alpha \Psi_0^{(2)}(\pm 1) \phi_{22}(\pm 1) + \frac{\mu_1}{R_e} \xi_{22}^{(1)}(\pm 1) \\ &= \pm \frac{2 + \mu_1}{4R_e} (\alpha^2 \phi_1^{(2)}(\pm 1) - \phi_1^{(4)}(\pm 1)) - \frac{(2 + \mu_1)\Psi_0^{(5)}(\pm 1)}{8R_e} \\ &+ 2i\alpha [(\phi_1^{(1)}(\pm 1))^2 - \phi_1(\pm 1)\phi_1^{(2)}(\pm 1) \mp \phi_1^{(2)}(\pm 1)]/4 \\ &- \frac{i\alpha}{2} \Psi_0^{(3)}(\pm 1)\phi_1(\pm 1) - \frac{\mu_1}{2R_e} \left(\xi_1^{(2)}(\pm 1) \pm \frac{\nu_0^{(2)}(\pm 1)}{2} \right). \end{aligned}$$

Appendix B.

The solutions to (3.4)–(3.5) are

$$\begin{aligned} \phi_1(y) &= A_3 \sinh \alpha y + A_4 \sinh \beta y + a_1 A_1 \sinh r_1 y + a_2 A_2 \sinh r_2 y, \\ \xi_1(y) &= A_1 \sinh r_1 y + A_2 \sinh r_2 y, \end{aligned}$$

where

$$\begin{aligned} A_3 &= \frac{-\bar{\delta}_1 + a_1 A_1 r_1 (r_1^2 - \beta^2) \cosh r_1 + a_2 A_2 r_2 (r_2^2 - \beta^2) \cosh r_2}{\alpha(\beta^2 - \alpha^2) \cosh \alpha}, \\ A_4 &= \frac{\bar{\delta}_1 - a_1 A_1 r_1 (r_1^2 - \beta^2) \cosh r_1 - a_2 A_2 r_2 (r_2^2 - \beta^2) \cosh r_2}{\beta(\beta^2 - \alpha^2) \cosh \beta}, \\ a_1 &= -2N^2/(r_1^2 - \beta^2), \quad a_2 = -2N^2/(r_2^2 - \beta^2), \\ A_1 &= R_e N^2 M^2 (\sinh r_2)/2d_1, \quad A_2 = -R_e N^2 M^2 (\sinh r_1)/2d_1, \\ d_1 &= (r_1^3 + (T_1 - T_2 - \alpha^2)r_1) \sinh r_2 \cosh r_1 \\ &\quad - (r_2^3 + (T_1 - T_2 - \alpha^2)r_2) \sinh r_1 \cosh r_2, \\ \bar{\delta}_1 &= R\delta_1 - 2N^2(r_1 A_1 \cosh r_1 + r_2 A_2 \cosh r_2), \\ r_1 &= \left(\left(-X_1 + \sqrt{X_1^2 - 4X_2} \right) / 2 \right)^{1/2}, \quad r_2 = \left(\left(-X_1 - \sqrt{X_1^2 - 4X_2} \right) / 2 \right)^{1/2}, \\ X_1 &= T_1 - T_2 - (\alpha^2 + \beta^2), \quad X_2 = \alpha^2 \beta^2 - T_1 \alpha^2 + T_2 \beta^2, \\ T_1 &= N^4 M^2 / (1 - N^2), \quad T_2 = N^2 M^2 / (1 - N^2) \quad \text{and} \quad \beta^2 = \alpha^2 - 2i\alpha R_e / (2 + \mu_1). \end{aligned}$$

The solutions to (3.6)–(3.7) are

$$\begin{aligned} \phi_{20}^{(1)}(y) &= G_1(y) - 2N^2G_2(y) - \frac{2NC_2}{M} \cosh(NMy) + \frac{C_1y^2}{2(1 - N^2)} + C_3, \\ \xi_{20}(y) &= C_2 \sinh(NMy) + f(y) - \frac{C_1y}{2(1 - N^2)}, \end{aligned}$$

where

$$C_1 = \frac{i\alpha R_e}{2 + \mu_1} D_3 + \frac{\alpha^2}{2} D_1 - \frac{1}{2} D_4 - N^2 D_5,$$

$$C_2 = \frac{C_1 - 2(1 - N^2)(f(1) + 0.5D_2)}{2(1 - N^2) \sinh(NM)},$$

$$C_3 = -0.5D_1 - G_1(1) + 2N^2G_2(1) + \frac{2NC_2}{M} \cosh(NM) - \frac{1}{2(1 - N^2)} C_1,$$

$$D_1 = \phi_1^{*(2)}(1) + \phi_1^{(2)}(1), \quad D_2 = \xi_1^{*(1)}(1) + \xi_1^{(1)}(1), \quad D_3 = \phi_1^{*(2)}(1) - \phi_1^{(2)}(1),$$

$$D_4 = \phi_1^{*(4)}(1) + \phi_1^{(4)}(1), \quad D_5 = \xi_1^{*(2)}(1) + \xi_1^{(2)}(1),$$

$$G_2(y) = \int f(y) dy, \quad G_1(y) = \frac{-i\alpha R_e}{2 + \mu_1} \int (\phi_1(y)\phi_1^{*(2)}(y) - \phi_1^*(y)\phi_1^{(2)}(y)) dy$$

and

$$\begin{aligned} f(y) &= -\frac{2i\alpha R_e N^2 M^2}{(2 + \mu_1)(1 - N^2)} \left[A_3 A_4^* (\beta^{*2} - \alpha^2) F(\alpha, \beta^*) \right. \\ &\quad + A_3 A_1^* a_1^* (r_1^{*2} - \alpha^2) F(\alpha, r_1^*) + A_3 A_2^* a_2^* (r_2^{*2} - \alpha^2) F(\alpha, r_2^*) \\ &\quad + A_4 A_3^* (\alpha^2 - \beta^2) F(\alpha, \beta) + A_4 A_4^* (\beta^{*2} - \beta^2) F(\beta, \beta^*) \\ &\quad + A_4 A_1^* a_1^* (r_1^{*2} - \beta^2) F(\beta, r_1^*) + A_4 A_2^* a_2^* (r_2^{*2} - \beta^2) F(\beta, r_2^*) \\ &\quad + A_1 A_3^* a_1 (\alpha^2 - r_1^2) F(\alpha, r_1) + A_4 A_4^* a_1 (\beta^{*2} - r_1^2) F(r_1, \beta^*) \\ &\quad + A_1 A_1^* a_1 a_1^* (r_1^{*2} - r_1^2) F(r_1, r_1^*) + A_1 A_2^* a_1 a_2^* (r_2^{*2} - r_1^2) F(r_1, r_2^*) \\ &\quad + A_2 A_3^* a_2 (\alpha^2 - r_2^2) F(\alpha, r_2) + A_2 A_4^* a_2 (\beta^{*2} - r_2^2) F(r_2, \beta^*) \\ &\quad \left. + A_2 A_1^* a_2 a_1^* (r_1^{*2} - r_2^2) F(r_2, r_1^*) + A_2 A_2^* a_2 a_2^* (r_2^{*2} - r_2^2) F(r_2, r_2^*) \right], \\ F(A, B) &= \frac{\sinh((A + B)y)}{(A + B)[(A + B)^2 - N^2 M^2]} - \frac{\sinh((A - B)y)}{(A - B)[(A - B)^2 - N^2 M^2]}. \end{aligned}$$

References

- [1] T. Ariman, M. A. Turk and N. D. Sylvester, “Microcontinuum fluid mechanics. A review”, *Int. J. Engng. Sci.* **11** (1973) 905–930.
- [2] T. Ariman, M. A. Turk and N. D. Sylvester, “Applications of microcontinuum fluid mechanics”, *Int. J. Engng. Sci.* **12** (1974) 273–293.

- [3] G. Böhme and R. Friedrich, "Peristaltic flow of viscoelastic liquids", *J. Fluid Mech.* **128** (1983) 109–122.
- [4] T. D. Brown and T. K. Hung, "Computational and experimental investigations of two-dimensional nonlinear peristaltic flows", *J. Fluid Mech.* **83** (1977) 249–272.
- [5] J. C. Burns and T. Parkes, "Peristaltic motion", *J. Fluid Mech.* **29** (1969) 731–743.
- [6] A. C. Eringen, "Theory of micropolar fluids", *J. Math. Mech.* **16** (1966) 1–18.
- [7] A. C. Eringen, *Microcontinuum field theories. Vol. II: Fluent media* (Springer, New York, 2001).
- [8] Y. C. Fung and C. S. Yih, "Peristaltic transport", *Trans. ASME J. Appl. Mech.* **35** (1968) 669–675.
- [9] R. Girija Devi and R. Devanathan, "Peristaltic transport of micropolar fluid", *Proc. Indian Acad. Sci.* **81(A)** (1975) 149–163.
- [10] M. Y. Jaffrin and A. H. Shapiro, "Peristaltic pumping", *Annual Rev. Fluid Mech.* **3** (1971) 13–36.
- [11] K. A. Kline and S. J. Allen, "Nonsteady flows of fluids with microstructure", *Phys. Fluids* **13** (1970) 263–270.
- [12] T. K. Mitra and S. N. Prasad, "On the influence of wall properties and Poiseuille flow in the peristalsis", *J. Biomechanics* **6** (1973) 681–693.
- [13] D. Philip and Peeyush Chandra, "Peristaltic transport of simple micro fluid", *Proc. Nat. Acad. Sci. India* **65(A)** (1995) 63–74.
- [14] J. Prakash and P. Sinha, "Squeeze film theory for micropolar fluids", *Tran. ASME J. Lubrication Tech.* **98** (1976) 139–144.
- [15] G. Radhakrishnamacharya, "Long wave length approximation to peristaltic motion of a power law fluid", *Rheol. Acta* **21** (1982) 30–35.
- [16] K. K. Raju and R. Devanathan, "Peristaltic motion of a non-Newtonian fluid. I", *Rheol. Acta* **11** (1972) 170–178.
- [17] B. V. Rathish Kumar and K. B. Naidu, "A numerical study of peristaltic flows", *Compt. Fluids* **24** (1995) 161–176.
- [18] K. P. Selverov and H. A. Stone, "Peristaltically driven channel flows with applications toward micromixing", *Phys. Fluids* **13** (2001) 1837–1859.
- [19] A. H. Shapiro, M. Y. Jaffrin and S. L. Weinberg, "Peristaltic pumping with long wavelength at low Reynolds number", *J. Fluid Mech.* **37** (1969) 799–825.
- [20] L. M. Srivastava, "Peristaltic transport of couple-stress fluid", *Rheol. Acta* **25** (1986) 638–641.
- [21] L. M. Srivastava and V. P. Srivastava, "Peristaltic transport of blood: Casson model. II", *J. Biomechanics* **17** (1984) 821–829.
- [22] S. Takabatake and K. Ayukawa, "Numerical study of two-dimensional peristaltic flows", *J. Fluid Mech.* **122** (1982) 439–465.
- [23] P. Tong and D. Vawter, "An analysis of peristaltic pumping", *Trans. ASME J. Appl. Mech.* **39** (1972) 857–862.
- [24] F. Yin and Y.C. Fung, "Comparison of theory and experiment in peristaltic transport", *J. Fluid Mech.* **47** (1971) 93–112.